International Journal of Fluid Power 4 (2003) No. 2 pp. 43-54

EVALUATION AND VALIDATION OF AN AIR SPRING ANALYTICAL MODEL

Giuseppe Quaglia and Andrea Guala

Department of Mechanics, Politecnico di Torino, Corso Duca degli Abruzzi 24, 10129 Torino, Italy
giuseppe.quaglia@polito.it

Abstract

The present paper responds to the following aim: to define a model, which can predict quite well the static characteristic of a bellow spring. In detail an analytical non-dimensional model of the bellow spring is obtained. It can describe the axial force and the effective area apart from its geometric size. The typical parameters of this model are spring geometrical ratio and number of convolutions. No detailed information about membrane characteristic is required. Internal volume and spring stiffness equations are then analytically derived.

At last a dynamic model of the spring is developed using the static characteristics previously defined. This tool would be useful for particular applications that involve dynamics as a keyword, such as vibration isolators, vehicle suspensions and actuators.

Keywords: air spring analytical model, non-dimensional model, bellow spring

This manuscript was received on 10 October 2002 and was accepted after revision for publication on 07 March 2003

1 Air Spring Description

The "bellow" type air spring is made up of an axial symmetric reinforced rubber membrane moulded in one or more superposed convolutions, and of two metallic flanges connected to its ends. Some examples of bellow springs are reported in Fig. 1. When the spring is working, the deformation of each convolution allows compression or rebound stroke. Springs with more than one convolution, usually to a maximum of three, are constructed to obtain high strokes without excessively straining membrane material.

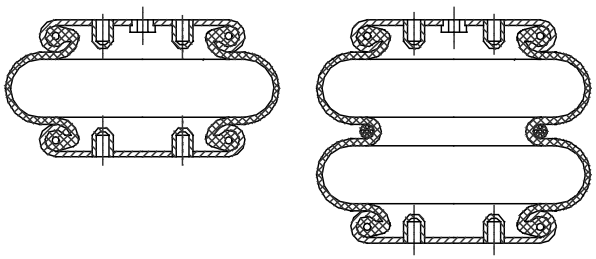

Fig. 1: *Commercial one- and two-convolution springs*

Air springs are intended as vibration isolation systems on stationary machinery, as vehicular suspensions and, at last, as mechanical actuators. In the first case the spring is used to limit forces transmitted to the foundation, if the machinery is a vibration source, or to limit the vibrations transmitted to the machinery if the foundation is a vibration source.

In the second case, that is vehicular suspension, the spring must assure comfort (i.e. isolation of vibration coming from the track to the vehicle), vehicle roll and yaw control and suitable contact forces between tyre and track, thus to guarantee an adequate trajectory control in every dynamic situation.

At last the third case, that is air spring used as actuator, regards the spring capability to exert forces on its ends even in transverse or angular off-axis configuration.

The characteristics of one spring strongly depend on its dimensions, number of convolutions and membrane material behaviour. Usually in commercial component catalogues, the exerted force F at constant pressure and the internal volume both versus spring height h are given. Figure 2 shows an example for a Firestone 224 spring with two convolutions.

The effective area, as defined in Eq. 1, is often reported instead of the F versus h graph.

$$A_{\mathrm{EFF}} = \frac{F}{p} \tag{1}$$

where p is the internal relative pressure.

Effective area is an ideal area on which the internal pressure p is supposed to act, balancing external force F.

This area is roughly independent of pressure *p*, because the membrane is not sensitively deformed by internal pressure. Starting from experimental data of *F* versus *h* shown in Fig. 2, it is usual to determine, through Eq. 1, the curve visible in Fig. 3.

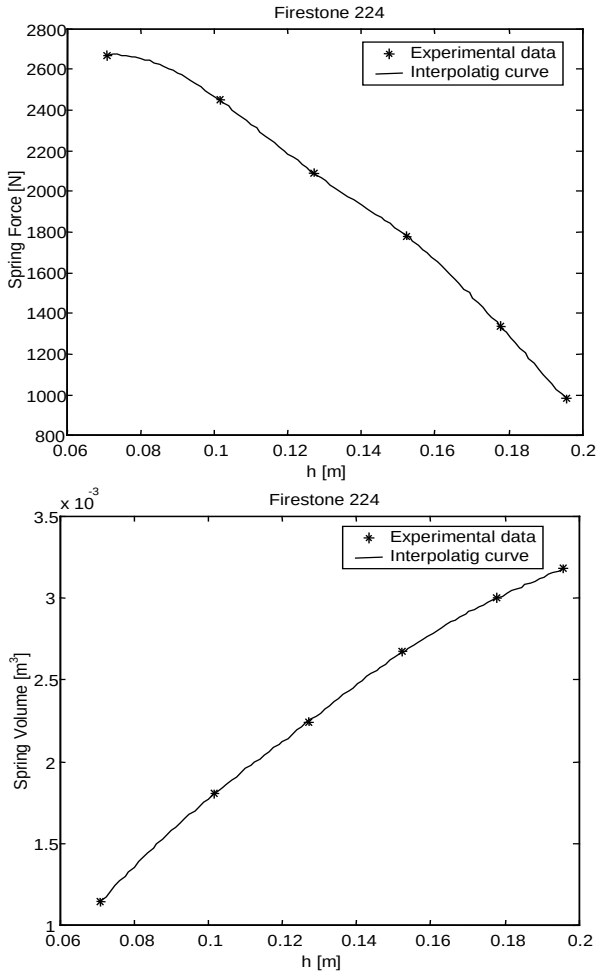

Fig. 2: *Firestone 224 two-convolution spring, static characteristic (p = 20 psi = 1.38 bar)*

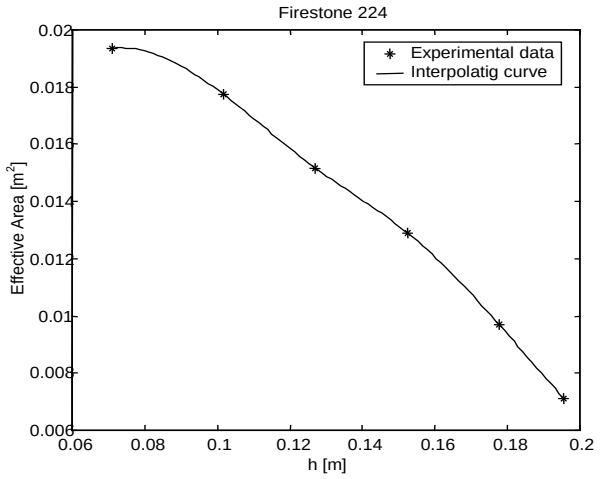

Fig. 3: *Firestone 224 spring effective area*

If possible, it is better to determine the effective area, averaging experimental data acquired in different pressure conditions. Through the curves shown in Fig. 2 and 3, it is possible to completely define the bellow spring.

Those curves can only be obtained via experiments or complex calculations (non-linear or FE models) based on a specific problem.

A vast number of papers about air springs can be found in literature, in spite of this no article presents a concise analytical method to analyse this kind of components.

A concise list of articles regarding air spring applications is reported in bibliography. The authors of the present paper have vastly studied the field of air-spring applications for vehicular purpose. Quaglia et al (1994) investigated a hydro-pneumatic suspension system, and in 1998 air suspension are used to control lateral dynamic of high-speed trains. A vast and deep analysis is developed in the field of pneumatically damped air suspensions which achieve damping effects using an external tank connected to the air spring through an orifice (Quaglia et al, 1999, 2000, 2001).

One of the forerunners about the study of gas suspensions (Cavanaugh, 1961) presented a vast synthesis. Detailed studies about energetic aspects and general-purpose air spring models are reported by Kornhauser et al (1993 and 1994).

Some examples of gas-springs in vehicular suspensions are reported by Bachrach et al (1983) and Toyofuku (1999). Examples of vibration isolation are given by Gee-Clough (1968) and Soliman et al (1966), and at last gas spring used as controlled force actuators are described by Stein (1995).

The present paper responds to the following aim: to define a model, which can predict quite well the static characteristic of a bellow spring. In detail an analytical non-dimensional model of the bellow spring is obtained. It can describe the axial force and the effective area apart from its geometric size. The typical parameters of this model are spring geometrical ratio and number of convolutions. No information about membrane characteristic is required. Internal volume and spring stiffness equations are then analytically derived.

At last a dynamic model of the spring is developed using the static characteristics previously defined. This tool would be useful for particular applications that involve dynamics as a keyword, such as vibration isolators, vehicle suspensions and actuators.

The scheme of a bellow spring is shown in Fig. 4, given that radius *r* has the same value for the end plates and for the internal rings and that the superposed convolutions are identical.

Referring to Fig. 4, for multiple-convolution springs it is possible to analyse one single convolution, obtaining *L*:

$$L = \frac{h - 2h_{\mathrm{F}} - (n-1)h_{\mathrm{A}}}{n} \qquad (2)$$

From here on the study will be done for single-convolution bellow, leaving the case of multiple-convolution to paragraph 4, where the model will be validated with experimental data.

The spring geometrical ratios are linked to the non-dimensional parameter δ, defined as follows:

$$\delta = \frac{L_F}{r} \tag{3}$$

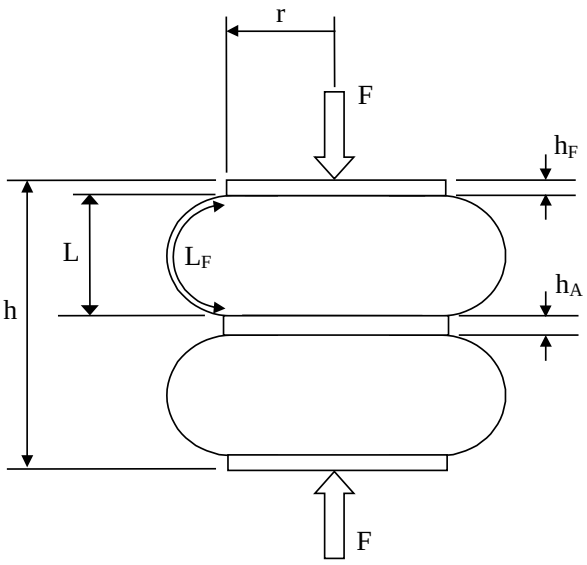

Fig. 4: *Bellow spring scheme*

A high δ stands for slim springs, while a low δ stands for squat springs, as it is shown in Fig. 5.

The model here developed can be used for designing purpose. It can predict the static characteristic and it can evidence, thanks to its non-dimensional formulation, the effect of dimension (r), dimension ratio ($\delta = L_F/r$), and number of convolution (n).

For spring choice purpose, the model could be useful to estimate the most suitable spring type (through parameters r, δ and n) for the specific application, before consulting any commercial catalogue.

At last the model can be used for spring dynamic analysis, that is important for vehicular suspension, vibration isolator and actuator design.

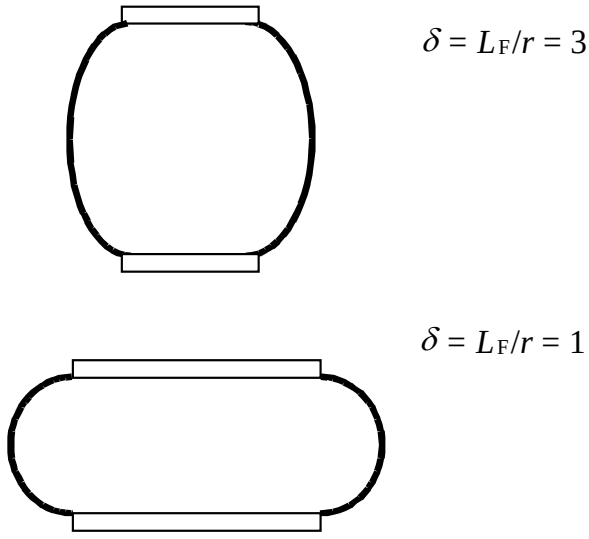

Fig. 5: *Air spring geometrical ratios*

2 Static Non-dimensional Ideal Model

The analytical static model must be able to express the force exerted by the spring as a function of its height, given internal pressure and geometrical ratio, (δ). Equilibrium equations of simplified geometry membrane and end plates are used.

The model is based on the following simplifying hypotheses:

- the membrane has a circular contour with curvature radius R, in longitudinal sections;
- the membrane stress distribution can be approximated transforming the closed axial symmetric contour in an open surface with the same longitudinal contour (as shown in Fig. 6) and assuming infinite fibres axial stiffness, while membrane circumferential stiffness is negligible.

These hypotheses lead to a significant analytical simplification. However, the comparison of analytical results and data from a manufacturer, for a number of commercial springs, is presented in paragraph 3. It shows the soundness of initial assumptions together with further simplifications used in paragraph 2.1.

2.1 Static Characteristic Derived from Equilibrium Equations

The analytical model for a single lobe air spring is developed. This model will be easily extended to multilobe springs through Eq. 2.

Longitudinal stress and geometrical aspects of the membrane can be obtained from Fig. 6, where the geometrical simplification is applied.

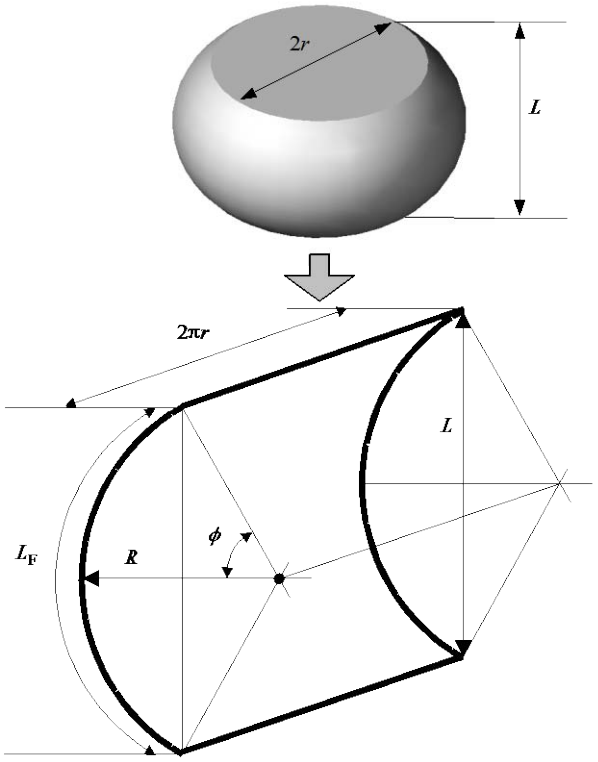

Fig. 6: *Simplified geometry obtained from axial symmetric convolution*

The forces acting on the simplified membrane con-

tour are shown in Fig. 7, leading to the following equilibrium equation:

$$p L\ 2\pi\ r = 2\ \tau\ t\ 2\pi\ r\ \sin\phi \tag{4}$$

so longitudinal axial stress τ is:

$$\tau = \frac{L\ p}{2\ t\ \sin\phi} \tag{5}$$

It is now clear that fiber axial stress τ increases as internal pressure p increases, and that it is a function of convolution length L and auxiliary angle ϕ. These two quantities, L and ϕ, are mutually dependent and this will be explained through geometrical considerations.

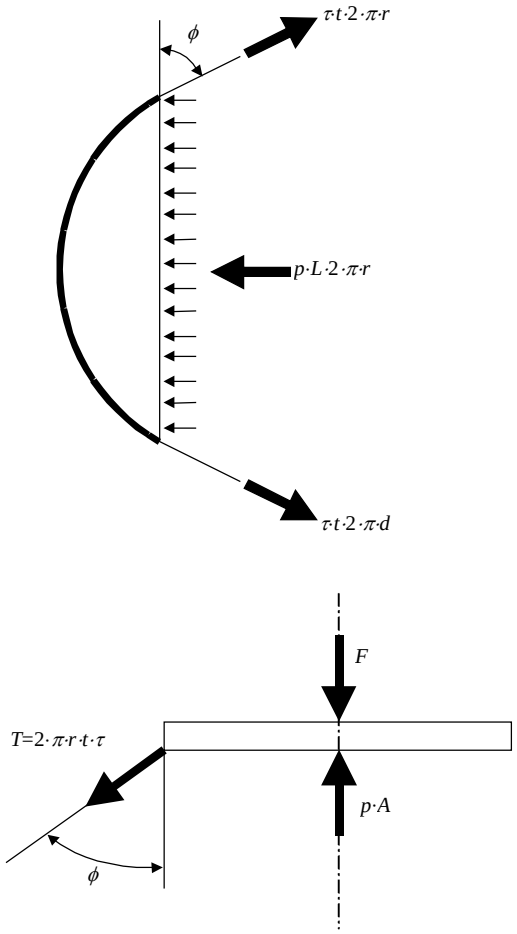

Fig. 7: *Equilibrium schemes of membrane and upper plate*

Figure 7 shows forces acting on the spring upper plate. Its axial equilibrium equation puts out the relations between external force F, internal pressure p and spring configuration, as a function of angle ϕ.

Vertical equilibrium equation is derived:

$$\tau\ t\ 2\pi r\ \cos\phi + F = p\ A \tag{6}$$

Putting Eq. 5 into Eq. 6, force F is obtained, with reference to angle ϕ and length L:

$$F = p\ A - \frac{L\ p}{\sin\phi}\ \pi r\ \cos\phi \tag{7}$$

Geometrical aspects

Equation 7 can be simplified finding the relation between auxiliary angle ϕ and length L.

Some considerations can be done looking at Fig. 6. First, fibers are considered longitudinally non-extendable, so fiber length L_F is constant during spring stroke. Second, a section of spring membrane is supposed to be a circular arc, with radius R. This arc subtends an angle, which value is 2ϕ.

Thus two geometrical relations are derived, the first from fiber infinite stiffness hypothesis:

$$R\ 2\phi = L_F \tag{8}$$

the second from trigonometric considerations:

$$R \cdot sin\phi = L/2 \tag{9}$$

using Eq. 8 and 9, it can be derived that:

$$L = L_F \frac{\sin\phi}{\phi} \tag{10}$$

So the substitution of Eq. 10 into 7 leads to:

$$F = p\ A - p\ \pi r^2 \frac{L_F}{r}\frac{\cos\phi}{\phi} \tag{11}$$

Introducing now F_A as the force exerted by internal pressure acting on end plate surface:

$$F_A = p\ A = p\ \pi r^2 \tag{12}$$

and geometrical ratio parameter $\delta = L_F/r$ into Eq. 11, the following non-linear equation system is obtained, using Eq. 10 for geometrical aspects:

$$\begin{cases} \dfrac{F}{F_A} = 1 - \delta\dfrac{\cos\phi}{\phi} \\ \dfrac{L}{L_F} = \dfrac{\sin\phi}{\phi} \end{cases} \tag{13}$$

This equation system expresses the non-dimensional spring force (F/F_A) versus non-dimensional spring length (L/L_F).

Remembering Eq. 8 and neglecting some mathematical calculations, it is possible to obtain from Eq. 13:

$$\frac{F}{F_A} \geq 0 \Leftrightarrow R\cos\phi \leq \frac{r}{2} \quad \text{PUSHING}$$

$$\frac{F}{F_A} < 0 \Leftrightarrow R\cos\phi > \frac{r}{2} \quad \text{PULLING}$$

these relations say that until the centre of the circular membrane contour is outside the circle of radius $r/2$ the spring pushes, in the other case he spring can only exert a pulling force.

In Eq. 13 auxiliary angle ϕ is still used to link the two equations. It is not possible to find one single equation to express non-dimensional force versus non-dimensional length, because in the second equation auxiliary angle ϕ cannot be analytically derived, as a function of L/L_F.

Non-dimensional length function $y = y(\phi)$ is introduced:

$$y = \frac{L}{L_F} = \frac{\sin\phi}{\phi} \tag{14}$$

Function $y(\phi)$ cannot be analytically inverted, but it can be approximated with a reversible function $y_1(\phi)$. A quadratic expression is chosen:

$$y_1 = a\phi^2 + b \tag{15}$$

In order to calculate appropriate coefficients *a* and *b*, Eq. 15 must cross two points of the exact solution Eq. 14.

The first point is $\phi = 0$, which corresponds to maximum extension condition and cylindrical membrane shape (Fig. 8 left), from Eq. 14:

$$y(0) = 1 \tag{16}$$

having $y(0)=y_1(0)$ first coefficient is found to be $b=1$.

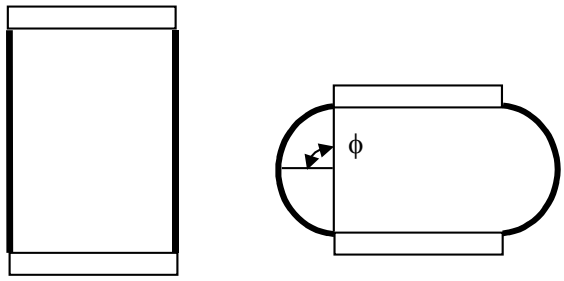

Fig. 8: *Spring in $\phi=0$ and $\phi=\pi/2$ conditions*

The second point is $\phi = \pi/2$, which corresponds to a half-circle membrane shape (Fig. 8 right), the exact solution says:

$$y(\pi/2) = \frac{2}{\pi} \tag{17}$$

having $y(\pi/2)=y_1(\pi/2)$, coefficient a is derived.

$$a = \frac{8-4\pi}{\pi^3} \tag{18}$$

Approximating function y_1 is then:

$$y_1 = \frac{8-4\pi}{\pi^3}\phi^2 + 1 = a\phi^2 + 1 \tag{19}$$

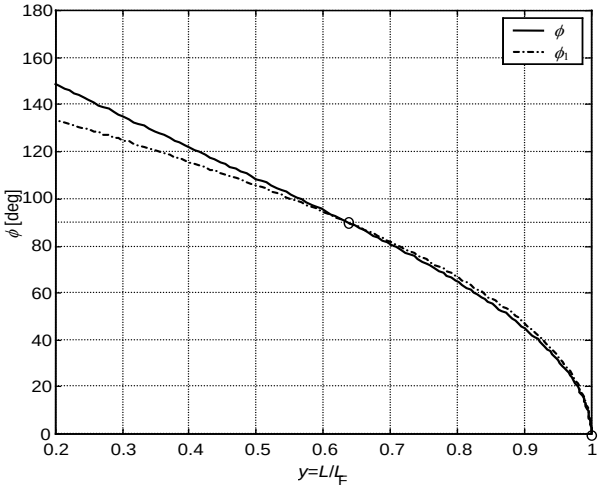

Fig. 9: *Comparison between ϕ and ϕ_1*

Inverse relation expresses ϕ versus spring length *L*:

$$\phi_1 = \sqrt{\frac{L/L_F - 1}{a}} \tag{20}$$

A comparison between exact Eq. 11 and approximate Eq. 20 solution can be seen in Fig. 9.

Figure 9 shows that the difference is always less than ±5° when the spring works in the range $L \cong (0.4 \div 1)\, L_F$.

Inserting quadratic expression Eq. 20 into Eq. 13, non-dimesional force with respect of non-dimensional spring length y is directly obtained:

$$\frac{F}{F_A} \cong 1 - \delta \frac{\cos\left(\sqrt{\frac{\frac{L}{L_F} - 1}{a}}\right)}{\sqrt{\frac{\frac{L}{L_F} - 1}{a}}} \tag{21}$$

Equation 21 evidences that the static behaviour depends on non-dimensional parameter $\delta = L_F/r$, always positive, which stands for spring "slimness".

Figure 10 shows how the approximated characteristic Eq. 21 varies when parameter δ changes.

It is clear that all the curves cross one single point with co-ordinates $(2/\pi, 1)$. This configuration corresponds to auxiliary angle $\phi = \pi/2$. This means that $F = F_A$, in equilibrium Eq. 7, because stress τ vector has no vertical component, referring to Fig. 7.

When "slimness" parameter δ increases the curve slope increases and, as a consequence, the intersection with abscissa axis moves to the left.

This means that for high values of δ the spring starts to exert traction forces ($F < 0$) in a more contracted configuration. For infinite "slimness" δ force inversion point corresponds to $y = L/L_F = 2/\pi$ ($\phi = \pi/2$).

The simplified model described by Eq. 21 has an obvious limit: it says that if ϕ would be zero (or $L/L_F = 1$), the membrane curvature will be null, and traction

force F and stress τ will become infinite. This comes from the simplifying assumptions and puts in evidence that the model does not work properly when the spring is highly extended.

It is now necessary to compare the results given by Eq. 21 with experimental data, particularly from catalogues of commercial springs. Thus, to check the soundness of above hypotheses and simplifications.

Equation 21 represents the characteristic of effective area, defined in Eq. 1: pressure p is constant, so it can be stated that:

$$\frac{F}{F_A} = \frac{A_{EFF}}{A} \tag{22}$$

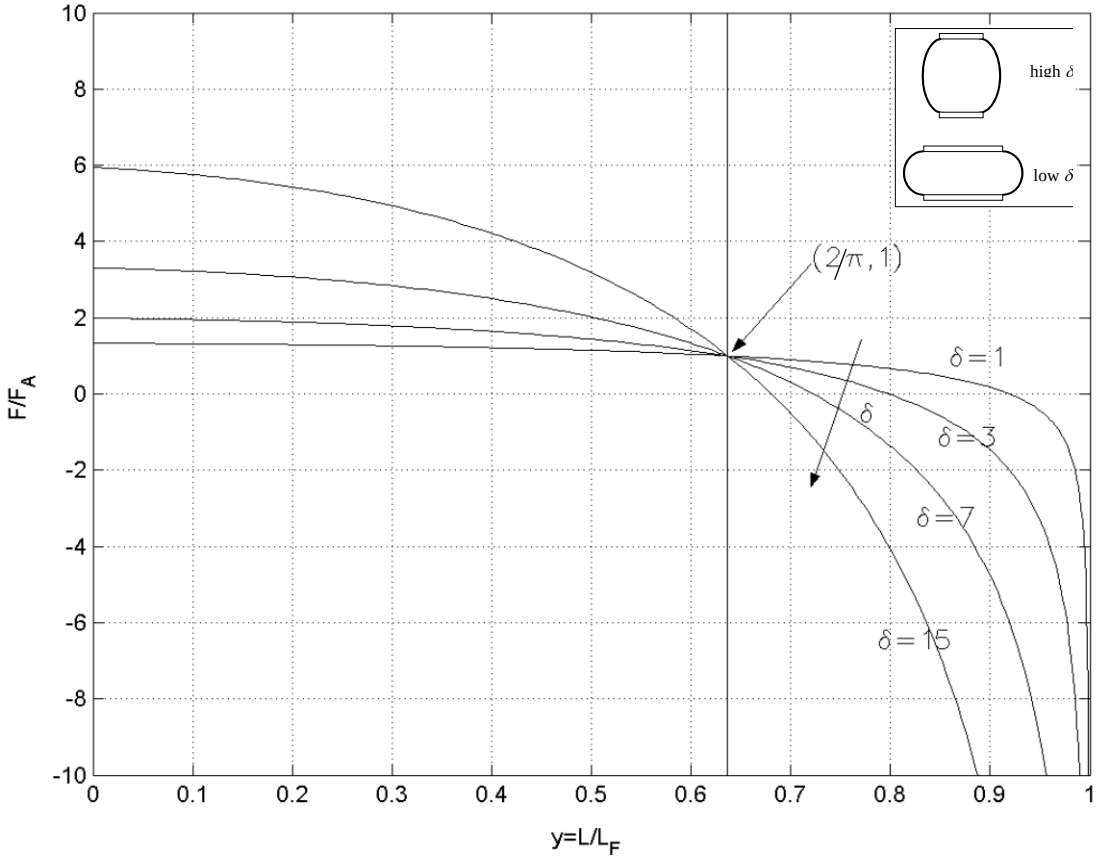

Fig. 10: *Force characteristic F/F_A versus non-dimensional length y*

3 Non-dimensional Model Validation with Data from Manufacturer

In this paragraph the validation of analytical model is presented, particularly referring to isobaric force curves and effective area curves, derived from commercial spring catalogues.

The comparison below reported regards air springs by CF-Gomma, but a larger investigation has involved components of the main producers. The whole validation activity gave results comparable to those reported here.

The parameters necessary to plot the analytical curve F versus L, using the following relation:

$$\frac{F}{F_A} = \frac{A_{EFF}}{A} \cong 1 - \delta \frac{\cos\left(\sqrt{\frac{L}{L_F} - 1}\right)}{\sqrt{\frac{L}{L_F} - 1}} \tag{21bis}$$

(where $\delta = \frac{L_F}{r}$, $F_A = p\ A$, $A = \pi\ r^2$), are here reported:

p = spring internal relative pressure,

r = end plate and internal ring radius,

L_F = constant longitudinal fiber length.

While p and r can be directly read in the spring data sheet, L_F is not immediately known, although it can be obtained with the appropriate equilibrium equation.

Figure 11-up shows the geometric configuration of one convolution when $\phi = \pi/2$, fiber axial stress direction is perpendicular to external force. This can be balanced only by $F_A = p\ A$.

These considerations also emerge in Fig. 10, because all the curves must cross the common point $y = L/L_F = 2/\pi$ and $F/F_A = 1$.

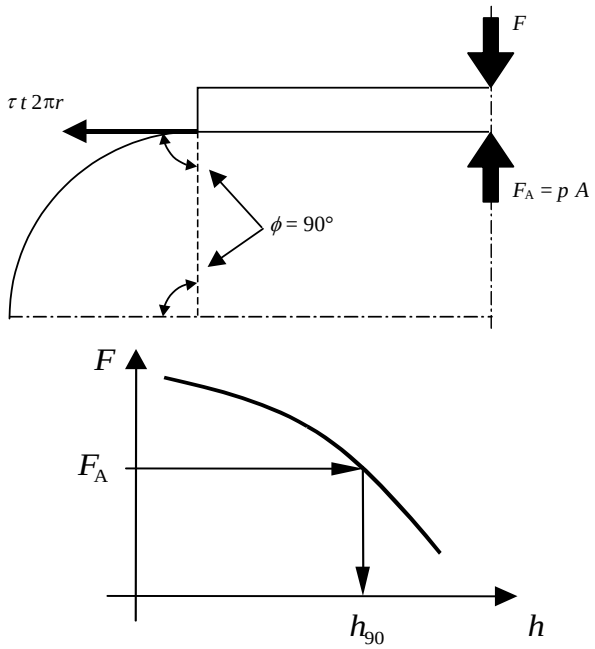

Fig. 11: *Spring configuration for $F = F_A$, and corresponding point on Force vs. height curve*

Starting from this consideration, it is possible, for any given isobaric characteristic, to derive height h_{90}, corresponding to $\phi = \pi/2$. In this case the exerted force F is equal to $F_A = p\,A$, this is schematically shown in Fig. 11 (right).

Given height h_{90}, the corresponding single lobe length L_{90} can be derived, for a spring having any number of convolution, from Eq. 2:

$$L_{90} = \frac{h_{90} - 2h_F - (n-1)h_A}{n} \qquad (2bis)$$

Fiber length can be consequently derived using Eq. 10:

$$L_F = \frac{\pi}{2} L_{90} \qquad (23)$$

Now all the necessary elements to solve Eq. 21bis are known. Therefore a comparison between analytical results and data from a commercial catalogue can be done.

In particular, it is decided to compare manufacturer and analytical curves of spring effective area, because this will be shown as an important element in the calculus of air-spring stiffness.

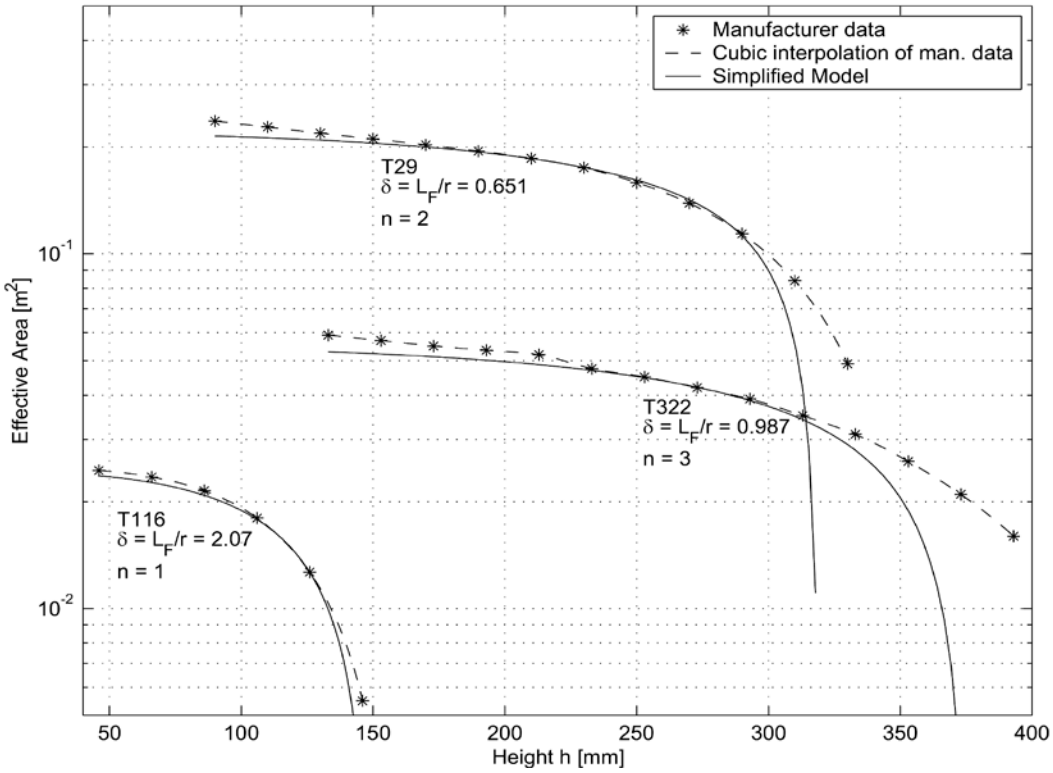

Fig. 12: *Comparison of manufacturer data and analytical curves*

Table 1: Catalogue data for the analysed springs

Spring T116	Spring T29	Spring T322
Single convolution (n = 1)	Double convolution (n = 2)	Triple convolution (n = 3)
Effective flange radius r = 67.5 mm	Effective flange radius r = 240 mm	Effective flange radius r = 114 mm

Geometrical ratio $\delta = L_F/r = 2.0653$		Geometrical ratio $\delta = L_F/r = 0.6507$		Geometrical ratio $\delta = L_F/r = 0.9868$	
Static height $h_{ST} = 100$ mm		Static height $h_{ST} = 190$ mm		Static height $h_{ST} = 260$ mm	
$\phi = \pi/2$	Height $h_{90} = 121$ mm	$\phi = \pi/2$	Height $h_{90} = 220$ mm	$\phi = \pi/2$	Height $h_{90} = 280$ mm
	Force ($p = 6$ bar) $F_A = 8.59$ kN		Force ($p = 6$ bar) $F_A = 108.5$ kN		Force ($p = 6$ bar) $F_A = 24.6$ kN

The curves are reported in Fig. 12 for three commercial models of air spring, with respectively one, two and three convolutions.

The catalogue data and the parameters used to describe the model are reported in Table 1 for the analysed springs.

In particular, static height h_{ST} is the nominal height suggested by the constructor. This value is quite close to h_{90}, this confirms that the membrane contour in this configuration is approximately half a circumference. For tested springs, the value of h_{ST} is always minor than h_{90}, therefore these springs are normally intended to work around a compressed configuration.

The analytical model well reproduces the manufacturer data, particularly for short strokes. When high strokes are reached, the membrane real shape does not exactly correspond to a circumference arc, because of the unpredictable deformations of rubber and of the membrane clamping in the upper and lower flanged joints. This leads to the visible divergence between analytical results and manufacturer curves.

4 Air-Spring Stiffness Analytical Evaluation

The analytical procedure to calculate the stiffness of an air-spring with n convolutions and constant air-mass is below reported, the notation refers to the two-lobed spring scheme in Fig. 13:

$$\begin{cases} F = p\ A_{EFF} \\ h = n\ L + 2h_F + (n-1)h_A \Rightarrow dh = n\ dL \\ K = -\dfrac{dF}{dh} = -\dfrac{1}{n}\dfrac{dF}{dL} = -\dfrac{1}{n}\dfrac{d(p\,A_{EFF})}{dL} = \\ = -\dfrac{1}{n}\left(\dfrac{dp}{dL}A_{EFF} + p\dfrac{dA_{EFF}}{dL}\right) \end{cases} \quad (24)$$

where p corresponds to relative pressure:

$$p = P - P_{AMB}.$$

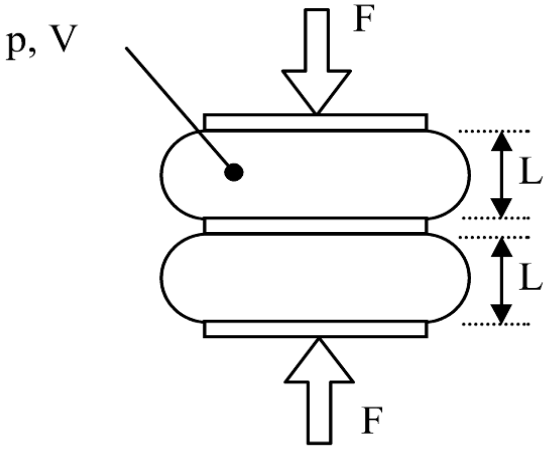

Fig. 13: *Scheme for air spring stiffness calculation*

The two derivative terms can be analytically obtained using the described simplified model.

Effective area derivative, can be obtained remembering Eq. 14, 20, 21 and 22:

$$\begin{cases} \dfrac{dA_{EFF}}{dL} = \dfrac{dA_{EFF}}{d\phi}\dfrac{d\phi}{dy}\dfrac{dy}{dL} \cong \\ = \dfrac{dA_{EFF}}{d\phi_1}\dfrac{d\phi_1}{dy}\dfrac{dy}{dL} = \\ = [\ldots] = \dfrac{\pi\, r}{2a\phi_1}\left(\dfrac{\sin\phi_1}{\phi_1} + \dfrac{\cos\phi_1}{\phi_1^2}\right) \\ \phi \cong \phi_1 = \sqrt{\dfrac{L/L_F - 1}{a}} \end{cases} \quad (25)$$

Pressure derivative, under the hypothesis of polytrophic transformation of exponent γ and using subscript i for fluid initial conditions, is obtained:

$$\begin{cases} \dfrac{dp}{dL} = \dfrac{dP}{dL} = [\ldots] = \dfrac{-\gamma P_i V_i^{\gamma}}{V^{\gamma+1}}\dfrac{dV}{dL} \\ P = \dfrac{P_i V_i^{\gamma}}{V^{\gamma}} \end{cases} \quad (26)$$

If the analytical stiffness is calculated for the suggested static height h_{ST}, corresponding to subscript 0, the final relation is:

$$K_0 = -\frac{1}{n}\left(-\frac{\gamma P_0 A_{\mathrm{EFF0}}}{V_0}\left.\frac{dV}{dL}\right|_0 + \right.$$
$$\left. +\left(P_0 - P_{\mathrm{AMB}}\right)\left.\frac{dA_{\mathrm{EFF}}}{dL}\right|_0 \right) = K_{\mathrm{V}} + K_{\mathrm{A}} \qquad (27)$$

Two contributions to spring stiffness can be evidenced: one linked to volume variation, which is K_{V}, and the other linked to the effective area variation, which is K_{A}.

Referring to the definition of effective area, it is likely to state that:

$$\frac{1}{n}\left.\frac{dV}{dL}\right|_0 = \left.\frac{dV}{dh}\right|_0 \approx A_{\mathrm{EFF0}}$$

so the stiffness can be expressed as follows:

$$K_0 = -\left(-\frac{\gamma P_0 {A_{\mathrm{EFF0}}}^2}{V_0} + \right.$$
$$\left. +\frac{1}{n}\left(P_0 - P_{\mathrm{AMB}}\right)\left.\frac{dA_{\mathrm{EFF}}}{dL}\right|_0 \right) = K_{\mathrm{V}} + K_{\mathrm{A}} \qquad (28)$$

From here on, two ways can be taken. In the first case, this formula can be directly used to calculate the static height stiffness, extracting the necessary data from experimental curves of effective area and volume. In the second case, Eq. 28 together with Eq. 25 is used to determine the air-spring stiffness through the analytical definition of angle ϕ_0, corresponding to height h_{ST}. The approximated relation for ϕ is:

$$\phi_0 \cong \phi_{10} = \sqrt{\frac{L_0 / L_{\mathrm{F}} - 1}{a}} \qquad (20\text{bis})$$

L_0 can be obtained from h_{ST}:

$$L_0 = \frac{h_{\mathrm{ST}} - 2h_{\mathrm{F}} - (n-1)h_{\mathrm{A}}}{n} \qquad (2\text{bis})$$

Stiffness Eq. 28 can be evaluated once volume V_0 is analytically known. It can be obtained through the procedure reported in the following paragraph.

4.1 Air-spring Volume Analytical Expression

With reference to the volume of a circular cylindrical barrel, *Guldino*'s formula is used according to the above-described geometrical definitions. The following equation system is obtained, for a single lobe spring:

$$\begin{cases} V_{1\mathrm{CONV}} = 2\pi\left[\frac{L^3}{12} + \right. \\ \left. +\frac{L_{\mathrm{F}}^2}{4}\left(r - \frac{L_{\mathrm{F}}}{2}\frac{\cos\phi}{\phi}\right)\left(\frac{1}{\phi} - \frac{L}{L_{\mathrm{F}}}\frac{\cos\phi}{\phi}\right)\right] + \pi\, r^2 L \\ \phi \cong \phi_1 = \sqrt{\frac{L / L_{\mathrm{F}} - 1}{a}} \end{cases} \qquad (29)$$

For an air spring with n lobes, the relation found is:

$$V_{\mathrm{TOT}} = n\, V_{1\mathrm{CONV}} + (n-1)\pi\, r^2\, h_{\mathrm{A}} \qquad (30)$$

The flanges contribution to total volume is neglected, while the volume given by internal rings is considered.

4.2 Validation of Volume Approximation

The validation of volume analytical equation is developed with reference to data from the manufacturer of CF-Gomma T26 spring. The parameters reported in Table 2 are used in Eq. 29 and 30.

Table 2: Data for the analysed spring

Spring number of convolutions	n	2
Static height	h_{ST}	165 mm
End plates diameter	$d = 2r$	135 mm
Longitudinal fiber length	L_{F}	95.7 mm
Upper and lower plate height	h_{F}	20 mm
Internal ring height	h_{A}	25 mm

Analytical results and volume curves from the manufacturer are compared in Fig. 14. Catalogue data are quite well approximated. Analytical volumes are normally bigger than those from the manufacturer, but the difference is sufficiently small near the operating height h_{ST} = 165 mm.

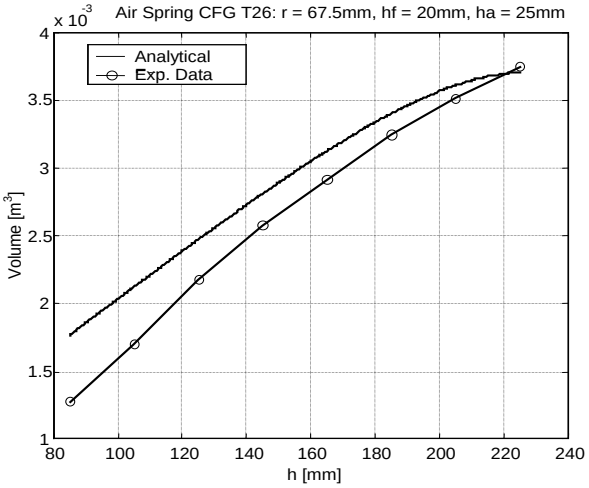

Fig. 14: *Analytical volume vs. data from the manufacturer*

Once volume mathematical expression is confirmed by manufacturer data spring stiffness around static height configuration can be evaluated.

4.2 Spring Stiffness Numerical Calculation

Stiffness evaluation can be done with reference to the above-derived equations. Supposing an internal pressure P_0 = 3 bar, the data reported in Table 3 are respectively obtained putting effective area data from the manufacturer and volume diagrams directly in Eq. 28 and using the above-described analytical procedure

through Eq. 25, 28, 29 and 30.

Table 3: Stiffness from manufacturer exp. data and analytical analysis (CF-GOMMA T26 spring)

	K_{EXP} [kN/m]	K_{AN} [kN/m]	Error % $[(K_{AN}-K_{EXP})/K_{EXP}]$
$\gamma = 1$	49.147	45.545	-7.33%
$\gamma = 1.4$	59.737	56.392	-5.6%

5 Air Spring Analytical Dynamic Modelling

The developed analytical model can be also used to simulate air spring dynamic behaviour. A block scheme of the air spring dynamic model is reported in Fig. 15. Model inputs are instantaneous spring height and entering mass flow, which can be null for some application. Starting from initial conditions, the model calculates the instantaneous exerted force.

In the scheme reported in Fig. 15, the two blocks containing the described analytical model are evidenced with grey colour, and can completely substitute experimental data mapping.

"Analytical Effective Area" block calculates the value of A_{EFF} from spring height, using Eq. 21bis,

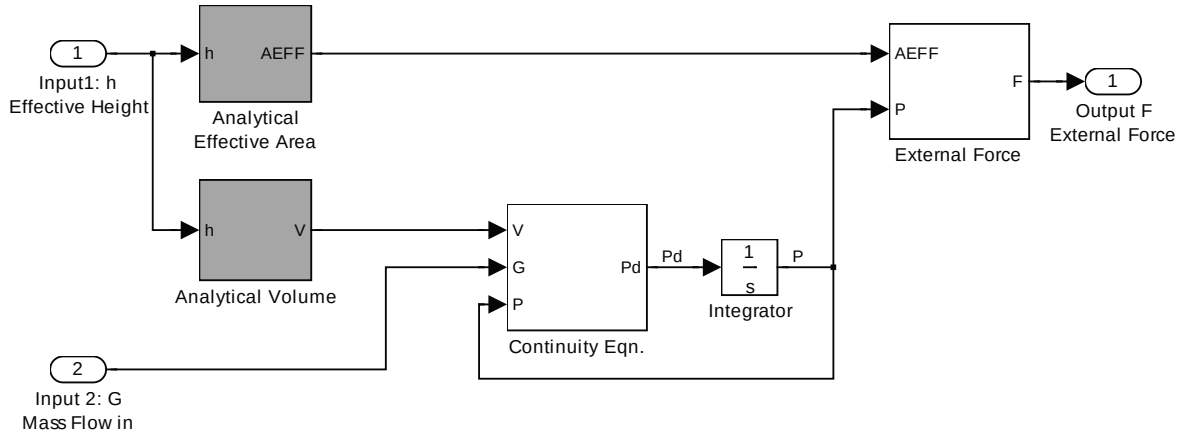

Fig. 15: *Block scheme of the air spring dynamic model*

"Analytical Volume" block calculates spring volume using Eq. 29.

"Continuity Equation" block is defined as follows:

$$\dot{P} = +\frac{\gamma R_G T_i}{V(h)}\left(\frac{P}{P_i}\right)^{\frac{\gamma-1}{\gamma}} G - \frac{\gamma P}{V(h)}\dot{V}(h) \qquad (31)$$

It calculates the spring internal pressure gradient with the fed-back absolute pressure instantaneous value and the numerically calculated volume time derivative. Numerical integration of the "Continuity Equation" output, leads to exerted force, obtained in "External Force" block, through the following equation:

$$F = (P - P_{AMB})\, A_{EFF} \qquad (32)$$

The described model can simulate the dynamic behaviour of any air spring once the "slimness" ratio δ, the flange radius r, the number of convolutions n, and the thickness of internal rings and end plates are known. No other experimental data is needed.

This can be particularly useful, because the influence of the main geometric parameter variation can be monitored when the spring is inserted in a complex model.

In order to give only an example of model's use the air spring in Fig. 16 is utilized as an actuator, to lift the sprung mass m.

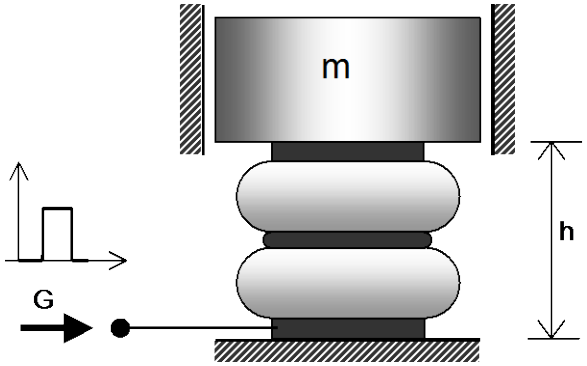

Fig. 16: *Test scheme for dynamic model*

In this case the dynamic model of Fig. 15 is a block of a complete model of the system that include the dynamic of the sprung mass and friction forces of the vertical guide. The model parameters, related to air spring CF-Gomma T26, are reported in the previous Table 2. The sprung mass m is equal to 30 kg. The simulation data and experimental data are compared in Fig. 17.

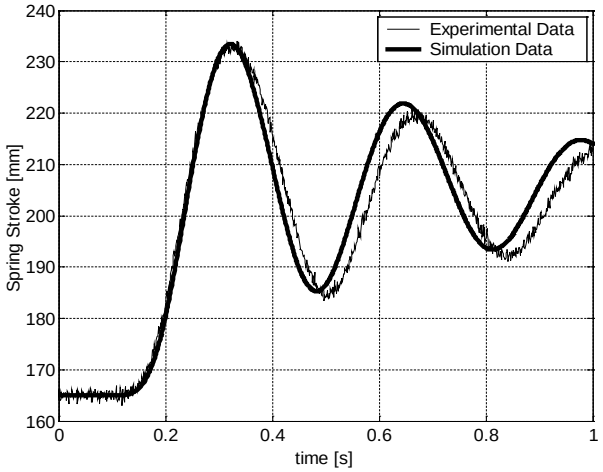

Fig. 17: *Simulation results of dynamic model*

The results shown in Fig. 17, confirm that the proposed model is a useful tools for preliminary design consideration. The restrictive hypotheses adopted in the model development and the limited number of model parameters, from one point of view leads to an easy to use and a general purpose model, but from the other a certain level of inaccuracy is implicit. To obtain more accurate results different and more complex models are required, but those models needs many detailed parameters, for example related to rubber's characteristics, and in this way they lose the analytical plainness.

6 Conclusions

The present paper gives some useful analytical tools to describe bellow air springs. In particular effective area and exerted force functions are derived in a non-dimensional form. The tools to analytically evaluate internal volume and spring stiffness are given as well. Finally, the structure of an air spring dynamic model is presented.

These proved to be good instruments both for preliminary spring design and for the analysis of complex mechanical systems with air springs.

Indeed the described analytical equations can predict the effect of spring geometrical parameters on its static and dynamic behaviour, on the other hand they form a complete model which can be used in specific applications, such as vehicular suspensions, vibration isolation and force actuation.

The comparison between model and experimental data of springs with different geometrical ratios, number of convolutions and producer, confirmed the strength of the obtained analytical equations.

Nomenclature

F	Spring exerted force	[N]
h	Spring height	[m]
h_F	Flanges height	[m]
h_A	Internal rings height	[m]
P	Spring internal absolute pressure	[Pa]
P_{AMB}	External ambient absolute pressure	[Pa]
p	Spring internal relative pressure	[Pa]
A_{EFF}	Spring effective area	[m^2]
L	Single convolution length	[m]
n	Spring number of convolutions	[-]
L_F	Membrane fiber length	[m]
r	External plates and internal rings radius	[m]
A	End plate area	[m^2]
F_A	Force exerted by pressure p vs. plates area	[N]
δ	Spring "slimness" non-dimensional parameter	[-]
t	Membrane thickness	[m]
R	Curvature radius	[m]
ϕ	Curvature arc half-angle	[rad]
τ	Membrane axial stress	[N/m^2]
a, b	Quadratic approximations constants	[-]
K	Spring stiffness	[N/m]
V	Spring internal volume	[m^3]
γ	Polythropic exponent	[-]
T	Air temperature	[°K]
R_G	Gas constant	[J/(kg·K)]
G	Spring input mass flow	[kg/s]

References

Quaglia, G., Mauro, S. and **Sorli, M.** 1994. Semi-Active Hydropneumatic Suspension. *Proc. 27th Int. Symposium on Automotive Technology & Automation ISATA*, pp. 173-180.

Quaglia, G., Sorli, M., Franco, W., Mauro, S., Giuzio, R. and **Vernillo, G.** 1998. Features of a Lateral Active Pneumatic Suspension in the High Speed Train ETR470. *Proc. 6th UK Mechatronics Forum Int. Conf. Mechatronics '98*, pp. 288-293.

Quaglia, G. and **Sorli, M.** 1999. Analysis of Vehicular Air Suspensions. *4th JHPS Int. Symp. on Fluid Power*, Tokyo, pp. 389-394**.**

Quaglia, G., Sorli, M. and **Guala, A.** 2000. Air Suspensions: Non Linear Analysis and Design Considerations. *2nd IFK Int. Fluidtechnisches Kolloquium*, Dresden, pp. 479-492.

Quaglia, G. and **Sorli, M.** 2000. Experimental and Theoretical Analysis of an Air Spring with Auxiliary Reservoir. *Proc. of the 6th International Symposium on Fluid Control Measurement and Visualization (FLUCOME 2000)*, Sherbrooke, Canada.

Quaglia, G. and **Sorli, M.** 2001. Air Suspension Dimensionless Analysis and Design Procedure. *Vehicle System Dynamics*, Vol. 6, pp. 443-475.

Cavanaugh, R. D. 1961. Air Suspension and Servo-controlled Pneumatic Isolation Systems. *Shock and*

Vibration Handbook, McGraw-Hill B.C., Chapter 33.

Kornhauser, A. A. and **Smith, J. L. Jr.** 1993. The Effects of Heat Transfer on Gas Spring Performance. *Journal of Energy Resource Technology*, Vol. 115, pp. 70-75.

Kornhauser, A. A. 1994. Dynamic Modelling of Gas Springs. *Trans. ASME: Journal of Dyn. Sys. Meas. and Cont.* 116, pp. 414-418.

Bachrach, B. I. and **Rivin, E.** 1983. Analysis of a Damped Pneumatic Spring. *Journal of Sound and Vibration*, Vol. 86 (2), pp. 191-197.

Toyofuku, K., Yamada, C., Kagawa, T. and **Fujita T.** 1999. Study on Dynamic Characteristic Analysis of Air Spring with Auxiliary Chamber. *JSAE review*, pp. 349-355.

Gee-Clough, D. and **Waller, R. A.** 1968. An Improved Self-Damped Pneumatic Isolator. *Journal Sound Vibration*, Vol. 8 (3), pp. 364-376.

Soliman, J. I. and **Tajer Ardabili, D.** 1966. Self-Damped Pneumatic Isolator for Variable Frequency Excitation. *Journal of Mechanical Engineering Science*, Vol. 8 (3).

Stein, G. J. 1995. Results of Investigation of an Electropneumatic Active Vibration Control System for a Driver's Seat. *Proc. Inst. Mech. Engrs. part D*, Vol. 209, pp. 227-234.

Giuseppe Quaglia
Born on January 27th 1964 in Pinerolo (Italy). 1989 - Degree in Mechanical Engineering. 1993 – PhD in Applied Mechanics - 1994 – Researcher in Applied Mechanics at the Dipartimento di Meccanica, Politecnico di Torino.
TEACHING
Applied Mechanics, Mechatonics, Mechanics of Automatic Machines, Fluid Automation
RESEARCH TOPICS
Mechatronics, mechanical systems control and regulation, innovative pneumatic systems and components, dynamic analysis of mechanical systems, robotics.

Andrea Guala
Born on September 10th 1973in Biella (Italy), graduated in Mechanical Engineering in 1999 at Politecnico di Torino. Since November 1999 he is attending the Ph.D. in Applied Mechanics in the Mechanical Department of the same Institute.
His research field mainly regards mechanical and mechatronic system dynamics, particularly linear and non-linear numerical simulation and field testing of systems and servo-systems including pneumatic and hydraulic components.